

# A Reliable 3D Laser Triangulation-based Scanner with a New Simple but Accurate Procedure for Finding Scanner Parameters

Ali Peiravi<sup>1</sup>, Behrai Taabbodi<sup>2</sup>

Ferdowsi University of Mashhad, Department of Electrical Engineering, School of Engineering, Mashhad IRAN  
Telephone number: (0098) 511-881-5100; Fax number: (0098) 511-8763302

<sup>1</sup>Ali\_peiravi@yahoo.com, <sup>2</sup>behrai@yahoo.com

**Abstract:** In this paper, a low occlusion laser triangulation 3D scanner based on two different color lasers and one color CCD camera is proposed. By placing a laser source in each side of the camera, occlusion problems are decreased to a minimum. Finding scanner parameters is one of the critical issues in 3D scanner accuracy. A new simple procedure is proposed to accurately find scanner parameters. [Journal of American Science 2010;6(5):80-85]. (ISSN: 1545-1003).

**Key words:** 3D scanner, laser triangulation, low occlusion, single camera

## 1. Introduction

Excellent properties of laser triangulation such as being a non-contact method, possessing a simple structure, having high precision and fast measurement speed have made it the best method to obtain three dimensional images. Laser triangulation-based 3D scanners are widely used in quality inspection, surface profile measurement, 3D modeling and reverse engineering applications.

The design of laser triangulation-based 3D scanners presents challenges in the design of optical routing, calculation of the laser spot, and system calibration. Moreover, issues such as laser reflective properties of the work-piece surface, speckle noise, occlusion and detecting the peak of the laser stripe using subpixel precision may affect the precision of the measurement.

A lot of work has been done by researchers to overcome these challenges, and several structures have been proposed as solutions for solving these problems [1]. A FIR filter approach for detecting the peak position of the laser stripe was presented in [2] and its performance was compared with other methods.

The occlusion problem can be somewhat reduced if either two lasers and one camera are used or two cameras and one laser are employed in the scanner. In this study, we use a red and a green laser plus a high resolution color camera to produce a low occlusion, high resolution scanner. If we compare this system with a scanner which uses two cameras and one laser, the two laser scanner has benefits such as a lower price, less complexity, and lower computing to prepare a 3D image. A new simple procedure for accurate calculation of scanner parameters is also presented.

The paper is organized as follows. In the following section, the basic principles of laser triangulation are reviewed. In the third section, our system structure for low occlusion is presented and its

advantages are introduced. In the fourth section, camera calibration and the procedure for finding the parameters are introduced. In the fifth section, the main parts making up the proposed system are introduced. In the sixth section, results of scanning an object and scanner parameters are presented. The last section is conclusions.

## 2. The basic principles of laser triangulation

Laser triangulation is based on the projection of a laser over an object and the image is captured by a digital camera. The 3d position of the laser beam over the object can be calculated by trigonometry, if we know the distance between the laser source and the camera (called baseline) and the angle between the baseline and the laser beam. An example of the triangulation system configuration is shown in Figure 1.

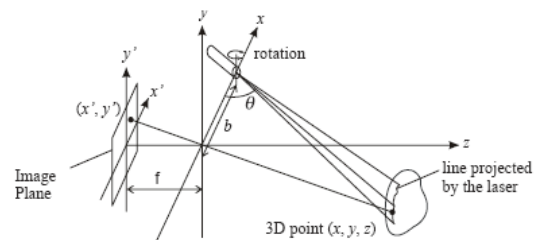


Figure 1. Example of triangulation system adopted from [3]

The coordinate  $(x,y,z)$  of a 3D point in real space which is projected onto the image pixel  $(x', y')$  can be found from equations (1), (2) and (3):

$$x = \frac{bx'}{f \cot \theta - x'} \quad (1)$$

$$y = \frac{by'}{f \cot \theta - x'} \quad (2)$$

$$z = \frac{bf}{f \cot \theta - x'} \quad (3)$$

where  $b$  is baseline,  $\theta$  is laser beam angle and  $f$  is the focal length [3].

### 3. System structure and its advantages

Our scanner structure is designed with the aim of high reliability, high resolution measurement, minimum occlusion problem, medium scan size, simple architecture and a low price.

Usually in many projects two cameras with two different fields of view are used to decrease the occlusion problem as shown in Figure 2. However, this increase the complexity and price of the scanner because we need two cameras and more computational expense for processing the data for the duplicate volume of picture data. Moreover, this additional hardware complexity would reduce the overall reliability of the system.

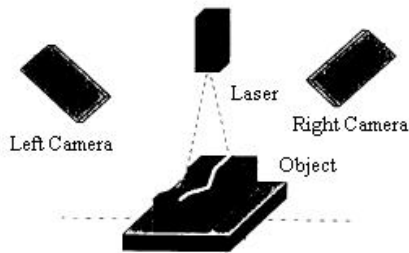


Figure 2. Laser triangulation 3d scanner with two cameras and one laser adopted from [4].

The use of two lasers with red and green color and one color camera is proposed in this paper to increase the overall system reliability. The lasers are placed on different sides of the camera. This architecture minimizes the occlusion problem. The reason for using different laser colors is to employ full size of image sensor for each lasers beam completely. Park et al. [5] proposed a 3D scanner with dual same-color lasers on the left and the right sides of the camera. To avoid the ambiguity in the detection of the two lasers beams, they assigned lasers beams to certain angles so that they never intersect each other in the scanner's field of view. This means that nearly one half of the image sensor is used by each laser, and the resolution of the scanner is drastically reduced and the scanner's measurable depth is decreased. In our proposed design, since we use two lasers with red and green colors, we can distinguish their beams in the RGB color camera.

One may calculate the distance in the Z- axis using equation (3). The measurement error and the parameters which affect it are given by (4). Range error in triangulation-based laser scanner come from the

error in estimate of position of the laser on the image sensor. Equation (4) gives the uncertainly approximation in Z [6]

$$\delta z \approx \frac{z^2}{fb} \delta x' \quad (4)$$

where  $f$  is focal length,  $b$  is the baseline,  $\delta x'$  is uncertainty in the laser position and  $z$  is the distance of the scanner to the object.

From equation (4), it can be seen that the error measurement in Z decreases with an increase in the camera baseline and the focal length of the lens, but dramatically increases by any increase of the distance.

In order to reduce the  $\delta x'$  to a minimum, a 7.2 mega pixel camera was used in this study and the center of mass algorithm was employed to accurately find laser position.

Unfortunately, there is a trade off between range error minimization and other specifications of the scanner such as reduction of occlusion problem and maximization of the camera's field of view. Thus, in the scanner  $f$  and  $b$  cannot be made as large as desired. The baseline is limited by the occlusion problem since occlusion increases with increasing  $b$ , and  $f$  is limited by the camera's field of view since the camera's field of view decreases with increasing  $f$ . In the proposed scanner design, we set the camera as near as possible to the object that we wish to scan.

Setting the camera very close to the object will lead to a small field of view for the scanner. However, we have solved this problem by moving the camera and the lasers together using an accurate linear motion system and preserved the scanner's field of view to maintain a high precision measurement.

### 4. Camera calibration and finding scanner parameters

Camera calibration and setting scanner parameters directly affect the scanner's precision. We need to calibrate the camera for its intrinsic parameters such as lens distortion. Also scanner parameters such as camera and laser baseline, laser beam angle, camera focal length, laser tilt versus camera Y axis and the angle between camera X axis and scanner linear motion system should exactly be set to accurately find 3D position of laser stripe on the object.

There are a lot of published papers about camera calibration [7]. However, our new procedure to find scanner parameters is very simple and there is no need for any mechanical calibration gages or any calibration points with exactly known position in three dimensions. The laser beam illumination on the flat table of the scanner with good reflectance properties is used for calculation of major scanner parameters, and sub-pixel resolution can be employed to find parameters with

high precision results. Also in our procedure we consider all of scanner details which cause accurate result in scanning.

In the proposed procedure, we use photogrammetry to find some of the parameters in order to calculate laser beam angle. Accurate lithography film is used for reference of measurements. The film is shown in Figure 3.

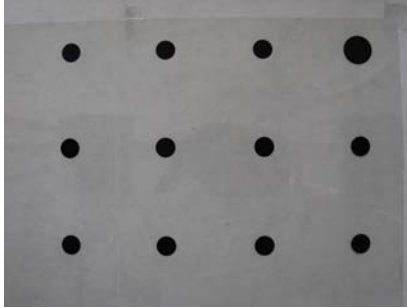


Figure 3. Picture of the lithography film. (Distances between the centers of the circles are 50mm)

Since the camera and the lasers are placed on the linear motion system with the capability of moving in the X and Z axes, we can use the Z axis to calculate the laser beam angle by taking two pictures with the camera. We first turn on the lasers and paste the film on the scanner table. Then we take two pictures. We take one picture when the Z position of the motion system is at  $z_1$  and take the second picture when it is at  $z_2$ . Then we process the two pictures and find the distance between the centers of the laser stripes in the two pictures with consideration of the fixed film in the pictures and the known center positions of the circles on it. Thus, we can calculate the laser beam angle using equation (5):

$$\theta = \cot^{-1}\left(\frac{\Delta x}{\Delta z}\right) \tag{5}$$

where  $\theta$  is the laser beam angle,  $\Delta x$  is the distance between the centers of the two laser stripes in two pictures and  $\Delta z = z_2 - z_1$ .

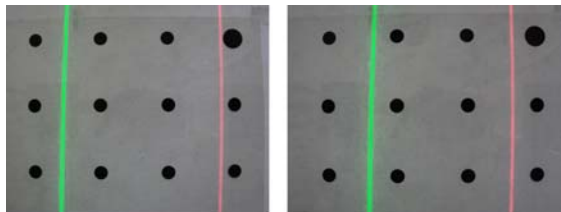


Figure 4. Two pictures which are used to calculate the laser beam angle.

Laser tilt versus camera Y axis is one of the other parameters of the scanner which should be considered.

For accurate scanning, it is necessary that the laser stripe be parallel with the Y axis of the camera. This situation needs very precise assembling of scanner parts. However, we can compensate the laser tilt instead of having precision assembly of the system. The laser tilt can be calculated with our accurate lithography film and photogrammetry method, as shown in Fig. 5. Equations (6) and (7) show the laser stripe tilt compensation.

$$Tilt = \frac{x_2 - x_1}{y_2 - y_1} \tag{6}$$

$$x' = x'_{WithLaserTilt} - Tilt \times y' \tag{7}$$

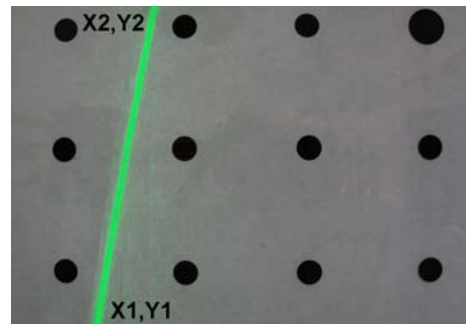


Figure 5. Compensation of the laser stripe tilt.

The angle between the x axis of the camera and the x axis of the scanner linear motion system is the third parameter which we calculate by using photogrammetry. If the angle is not equal to zero, we should compensate the results of the process for each stripe with equations (8) and (9):

$$X = y \sin \alpha + x \cos \alpha \tag{8}$$

$$Y = y \cos \alpha - x \sin \alpha \tag{9}$$

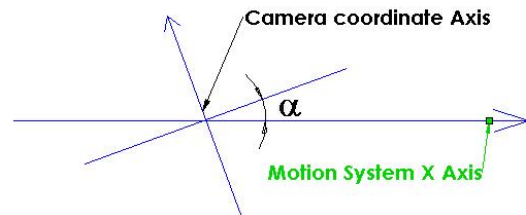


Figure 6. The angle between the x axis of the camera and the x axis of the scanner linear motion system.

To calculate the angle  $\alpha$ , we first calibrate the camera with the lithography film as shown in Figure 3. Then we change the film with a new one shown in Figure 7. Then we take two pictures with displacement of  $\Delta l$  in the x axis of the linear motion system. The calculation of the angle  $\alpha$  is given in (10):

$$\alpha = \sin^{-1}\left(\frac{\Delta y}{\Delta l}\right) \quad (10)$$



Figure 7. Lithography film used for calculating the  $\alpha$  angle.

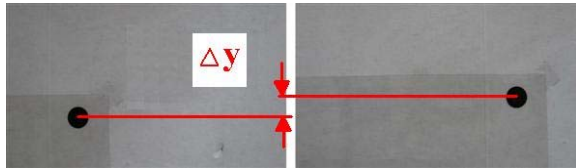


Figure 8. Two camera pictures are used to calculate the  $\alpha$  angle.

Finally, to calculate  $b$  (baseline) and  $f$  (focal length), we turn on the lasers and take 4 pictures with the camera in 4 different movements along the  $Z$  axis of the linear motion system from a position where the distance between the origin of coordinates of scanner and table of the scanner on the  $Z$  axis is  $z_0$ . These 4 movements take us to  $z_1, z_2, z_3$ , and  $z_4$  so the distances between the origin of the scanner and the table of the scanner on the  $Z$  axis are  $z_0 - z_1, z_0 - z_2, z_0 - z_3$ , and  $z_0 - z_4$  respectively. Note that we consider the sign of the 4 movements positive when they are in the direction of the scanner table.

So we write equation (3) for  $z_0 - z_1, z_0 - z_2, z_0 - z_3$  and  $z_0 - z_4$  as follows:

$$z_0 - z_1 = \frac{bf}{f \cot \theta - x'_A} \quad (11)$$

$$z_0 - z_2 = \frac{bf}{f \cot \theta - x'_B} \quad (12)$$

$$z_0 - z_3 = \frac{bf}{f \cot \theta - x'_C} \quad (13)$$

$$z_0 - z_4 = \frac{bf}{f \cot \theta - x'_D} \quad (14)$$

In the above equations, we know  $z_1, z_2, z_3, z_4, x'_A, x'_B, x'_C, x'_D, \theta$  and  $z_0, f, b$  are unknown. Then we can calculate  $f$  and  $b$  by using equations (15) and (16):

$$f = \frac{z_2 x'_B - z_1 x'_A + \frac{x'_B - x'_A}{x'_D - x'_C} (z_3 x'_C - z_4 x'_D)}{\cot \theta (z_2 - z_1 - \frac{x'_B - x'_A}{x'_D - x'_C} (z_4 - z_3))} \quad (15)$$

$$b = \frac{(z_2 - z_1)(f \cot \theta - x'_A)(f \cot \theta - x'_B)}{f(x'_B - x'_A)} \quad (16)$$

With the procedure explained above, all of the scanner parameters may be calculated and used for scanning.

### 5. Description of the system

A picture of the prototype of the system built is shown in Figure 9. The camera and the laser diodes are placed on a high accuracy Cartesian 3-Axis ball screw drive motion system with 0.05 mm resolution. Here, only the  $X$  and  $Z$  axes are used in the scanner. Two 5 mw linear red and green laser diodes with 650 nm and 532 nm wave length are placed on the right and left sides of the camera and one Sony DSC-H5 7.2 Mega pixels (3072 pixels x 2304 pixels x 24 bits color) camera is used.

### 6. A scanned case

To present an example, a computer mouse was scanned. Its photograph is shown in Figure 10. The point cloud models resulting from the green laser scan is shown in Figure 11, and the point cloud models resulting from the red laser scan is shown in Figure 12. The right side of the object did not scan well in the green laser scan because the occlusion problem happened. On the other hand, the left side of the scanned mouse did not scan well in the red laser scan due to the occlusion problem. However, a better point cloud model is produced by combining these two scans together as shown in Figure 13. Results of calculated scanner parameters are shown in Table 1.

### 7. Conclusions

In this paper, the design and implementation of a new 3D scanner is presented based on laser triangulation which has several advantages over existing systems. In this approach, two laser with different colors and one color CCD camera were used to minimize the occlusion problem and increase the overall system reliability. The proposed scanner is much cheaper and is less complex compared with the scanners which include two cameras and one laser. Also because two different color lasers are used, there

is no ambiguity in distinguishing between the two lasers and the full CCD has been used for each of the lasers.

Another advantage of our scanner is an appropriate field of view with a low range error. This was achieved by placing the scanner near the object to decrease the range error and by moving the camera and lasers together on the linear motion system to increase the field of view.

A new yet simple procedure is presented in this paper to accurately find the scanner parameters with sub-pixel resolution without any need for accurate mechanical gage or calibration points with known precise 3D position.

Table 1: Calculated scanner parameters

Red Laser Beam Angle	51.19
Green Laser Beam Angle	46.63
Red laser Tilt	0.0125
Green laser Tilt	0.0303
Red laser baseline	128.61 mm
Green laser baseline	180.95 mm
Focal length	6.62 mm
$\alpha$ angle	0.587

#### Acknowledgement

We would like to thank the Office of Vice Chancellor of Research and Technology of Ferdowsi University of Mashhad for their support of this research via the Grant Project 8146 (1387/5/17) that has assisted us in carrying out the research that led to the preparation of this manuscript.

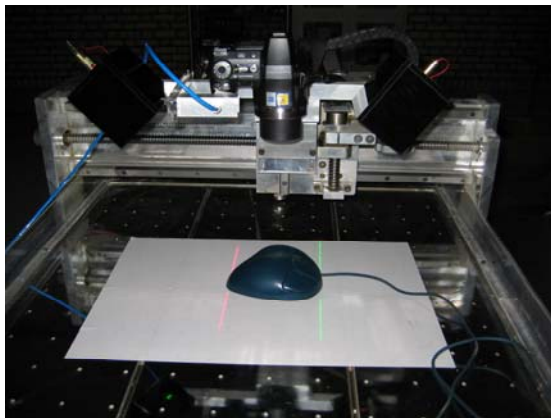


Figure 9. The prototype of the built system showing its architecture



Figure 10. Photograph of computer mouse which was scanned



Figure 11. Result of green laser scan.

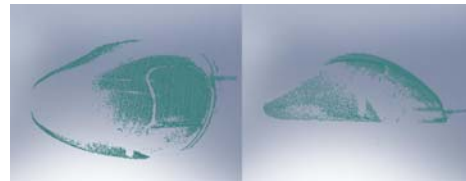


Figure 12. Result of red laser scan.

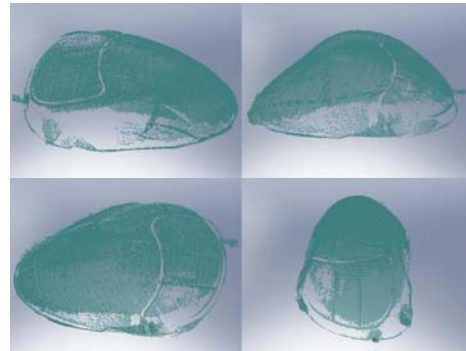


Figure 13. Result of combination of the red and green laser scans.

#### References

- [1] Lei Wang, Mei Bo, Jun Gao, Chun Sheng Ou, "A Novel double triangulation 3D camera", Proceedings of the 2006 IEEE International Conference on Information Acquisition, Aug. 20-23, 2006, Weihai, Shandong, China.
- [2] Josep Forest, Joaquim Salvi, Enric Cabruja and Carles Pous, "Laser stripe peak detector for 3D scanners. A FIR filter approach", IEEE Proceedings of the 17th International Conference on Pattern Recognition, ICPR 2004, Vol. 3, pp. 646 – 649, Aug. 2004.
- [3] Joao Guilherme D. M. Franca, Mario A. Gazziro, Alessandro N. Ide, Jose H. Saito, "A 3d scanning system based on laser triangulation

- and variable field of view", IEEE International Conference on Image Processing, ICIP 2005, Vol. 1, pp. 425-428, Sept. 2005.
- [4] P. Saint-Marc, J. L. Jezouin, and G. Medioni, "A versatile PC-based range finding system", IEEE Transactions on Robotics and Automation, Vol. 7, No. 2, pp. 250-256, Apr. 1991.
- [5] Johnny Park, Guilherme N. DeSouza and Avinash C. Kak, "Dual-beam structured-light scanning for 3-d object modeling", IEEE Proceedings of the Third International Conference on 3-D Digital Imaging and Modeling, pp. 65-72, 2001.
- [6] Fabrizio De Nisi, Fiorenzo Comper, Lorenzo Gonzo, Massimo Gottardi, David Stoppa, Andrea Simoni, and J.-Angelo Beraldin, "A CMOS sensor optimized for laser spot-position detection", IEEE Sensors Journal, Vol. 5, No. 6, pp. 1296-1304, Dec. 2005.
- [7] R. Y. Tsai, "A versatile camera calibration technique for high-accuracy 3-D machine vision metrology using off-the-shelf TV cameras and lenses", IEEE Journal of Robotics and Automation, Vol. 3, No. 4, pp. 323-344, Aug. 1987.

9/14/2009